Supplementary Materials

Mechanisms of imbalanced frontostriatal connectivity in obsessive-compulsive disorder

Sebastien Naze, Luke J. Hearne, James A. Roberts, Paula Sanz-Leon, Bjorn Burgher, Caitlin Hall, Saurabh Sonkusare, Zoie Nott, Leo Marcus, Emma Savage, Conor Robinson, Ye Ella Tian, Andrew Zalesky, Michael Breakspear, Luca Cocchi

Supplementary Text

Neuroimaging data preprocessing

Whole-brain echo-planar images (eyes open resting state) were acquired with the following parameters: voxel size = 2 mm^3, TR = 810 ms, multiband acceleration factor = 8, TE = 30 ms, flip angle = 53°, field of view (FoV) = 212 mm, 72 slices. Eye-open resting-state recordings lasted 11.9 minutes (880 volumes). Anterior-to-posterior and posterior-to-anterior spin-echo field maps were also acquired to correct for image distortions. Note that Harrison *et al.*[4] used a 4 minutes eye-closed resting-state paradigm on a 1.5T MRI scanner equipped with an 8-channel coil.

Structural brain images (MPRAGE GRAPPA2) were acquired with the following parameters: voxel size = 1 mm^3, TR = 1900 ms, TE = 2.98 ms, 256 slices, flip angle = 9°. Multi-shell diffusion-weighted images were acquired with a voxel size of 2 mm^3, 72 slices, FoV = 244 mm, TE = 84 ms, TR = 6200 ms, with anteroposterior phase encoding using 88 diffusion directions (b = 1000, b = 2950, and b = 3000 s/mm^2). Anterior-to-posterior and posterior-to-anterior field maps were also acquired to correct for image distortions.

Functional MRI

The data were skull stripped, corrected for susceptibility distortions, co-registered to the anatomical image and slice time corrected. Following this, denoising was conducted using ICA-FIX,[12] which involves identifying and removing nuisance signal components (derived from an independent component analysis) using a supervised classification algorithm.[31] After FIX-ICA denoising, the data were resampled to a standard template space (MNI152NLin2009cAsym). Resting-state data were subsequently detrended, regressed from

the global signal, temporally filtered (0.01-0.1 Hz), and scrubbed with FD threshold of 0.5 based on pre ICA-FIX motion estimation, ensuring an optimal trade-off between volume retention and noise removal (retention of *n*=97 subjects). Cortical activity was spatially smoothed with an 8 mm FWHM Gaussian filter. These pre-processing steps were identical for the data used in the DCM analyses, except that only a high pass filter was adopted (cut-off at 0.0078 Hz) and scrubbing was not performed to avoid spectral artefacts.

For the confirmatory analysis, cortical masks were derived from whole-brain resting-state data from 1080 healthy young adults included in the Human Connectome Project (HCP)[16]. The fMRI data was denoised using ICA-FIX,[12,31] spatially smoothed with 6 mm FWHM (full width at half maximum), and Wishart filtering, which is a PCA-based denoising method,[32] was applied to further improve the signal-to-noise ratio. These preprocessed fMRI time series were temporally concatenated across two runs (left-to-right and right-to-left phase encoding) acquired on day 1 (REST1), resulting in approximately 30 mins (2400 time points) of fMRI time series for FC estimation for each participant. Pearson correlation was computed between the mean time series across all voxels in the bilateral striatal seeds (see main text) and all gray matter voxels (n=164,850), yielding four FC maps for each participant (i.e., one map per cortical system). Individual FC maps were averaged across subjects and a threshold (> mean + 1 SD) of FC value was used to generate four binary masks corresponding to the four cortico-striatal systems of interest (Supplementary Fig. 1). Each cortical mask contained a similar number of voxels (approx. 30,000). Non-parametric inference was performed as described for the main analysis, with the difference that we adopted variable cluster thresholds (between t=2.5 and t=3.5) to confirm the stability of the results.

Supplementary References

31. Salimi-Khorshidi G, Douaud G, Beckmann CF, Glasser MF, Griffanti L, Smith SM. Automatic Denoising of Functional MRI Data: Combining Independent Component Analysis and Hierarchical Fusion of Classifiers. *Neuroimage.* 2014;90:449–68.
32. Glasser MF, Coalson TS, Bijsterbosch JD, *et al*. Using Temporal ICA to Selectively Remove Global Noise While Preserving Global Signal in Functional MRI Data. *Neuroimage.* 2018;181:692–717.

Frontostriatal system according to Shephard *et al.*[1]	Seed used from Di Martino *et al.*[14] (and Harrison *et al.*)[4] [x,y,z] MNI coordinates	Cortical region labels used from Schaefer *et al.*[13]
Ventral affective circuit	VSi (NAcc) [±9,9,−8]	OFC, PFClv, PFCv
Ventral cognitive circuit	VRP (vPut) [±20,12,-3]	PFCl, PFCm
Dorsal cognitive circuit	DC (dCaud) [±13,15,9]	PFCd, PFCld, PFCmp
Sensorimotor circuit	DCP (dPut) [±28,1,3])	Ins, SomMotB_S2

Supplementary Table 1: Mapping of frontostriatal systems. Each frontostriatal system is related to a striatal seed and its corresponding frontal region as suggested by Shephard *et al.*[1]. OFC: orbitofrontal cortex, PFC: prefrontal cortex, l: lateral, m: medial, d:dorsal, v:ventral, Ins: insula, SomMot: somato-motor cortex. Striatal seeds were taken from Di Martino *et al.*[14] (VSi: ventral striatum inferior, VRP: ventro-rostral putamen, DC: dorsal caudate, DCP: dorso-caudal putamen), and were adopted by Harrison *et al.*[4] using slightly different names (NAcc: Nucleus Accumbens, vPut: ventral putamen, dCaud: dorsal caudate, dPut: dorsal putamen).

Supplementary Figures

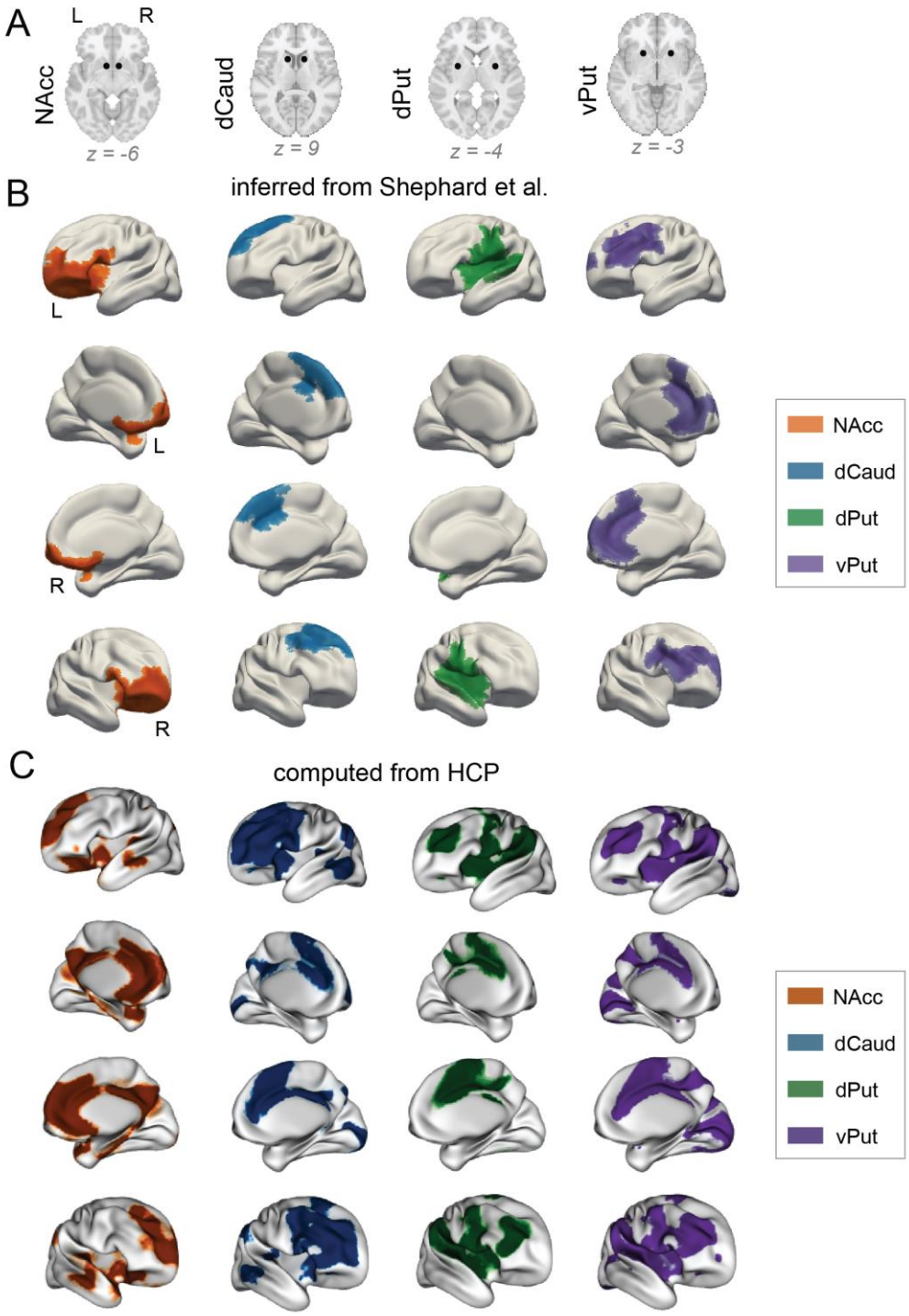

Supplementary Figure 1: Cortical regions defining the four frontostriatal systems of interest. (A) Seed locations of the four striatal regions of interest as per Di Martino *et al.*[14] and Harrison *et al.*[4]. NAcc: Nucleus Accumbens [±9,9,−8], dCaud: dorsal caudate [±13,15,9], dPut: dorsal putamen [±28,1,3], vPut: ventral putamen [±20,12,-3] ([x,y,z] in MNI coordinates). **(B)**

Frontal brain regions associated with the four striatal seeds from panel A, according to Shephard *et al.*[1] using Schaefer *et al.*[13] parcellation labels (Materials and Methods). L-R: left-right hemispheres. **(C)** Whole-brain cortical masks correlated with the four striatal seeds from panel A, using 1080 participants from the HCP (Supplementary Text).

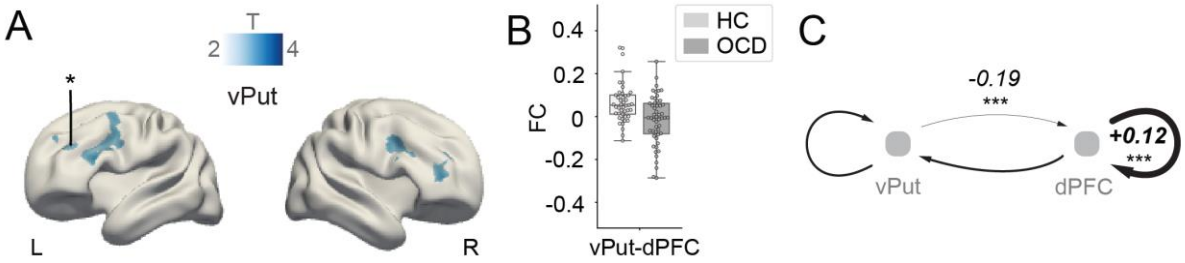

Supplementary Figure 2: Functional and effective connectivity differences in OCD versus healthy controls (HC) in the vPut-dPFC system. (A) Main effect of group in the absence of a group by hemisphere interaction: decreased functional connectivity in OCD (|T|>2.5). * p_{uncorr}<0.0005 at cluster level. R: Right hemisphere; L: Left hemisphere. **(B)** Pearson correlation values (FC) between fMRI signals in the seed regions and the highlighted cluster from panel A (*). Boxes extend from first to third quartile, whiskers span 1.5 of the interquartile range, and individuals' FC are marked by small circles **(C)** Group differences in effective connectivity between seed region and cortical cluster depicted by the star (*) in panel A. + (thick) and – (thin) signs (lines) indicate deviations relative to the mean across groups inferred through dynamic causal modelling. *** Posterior probability Pp>0.95 [very strong]. vPut: ventral putamen; dPFC: dorsal prefrontal cluster.

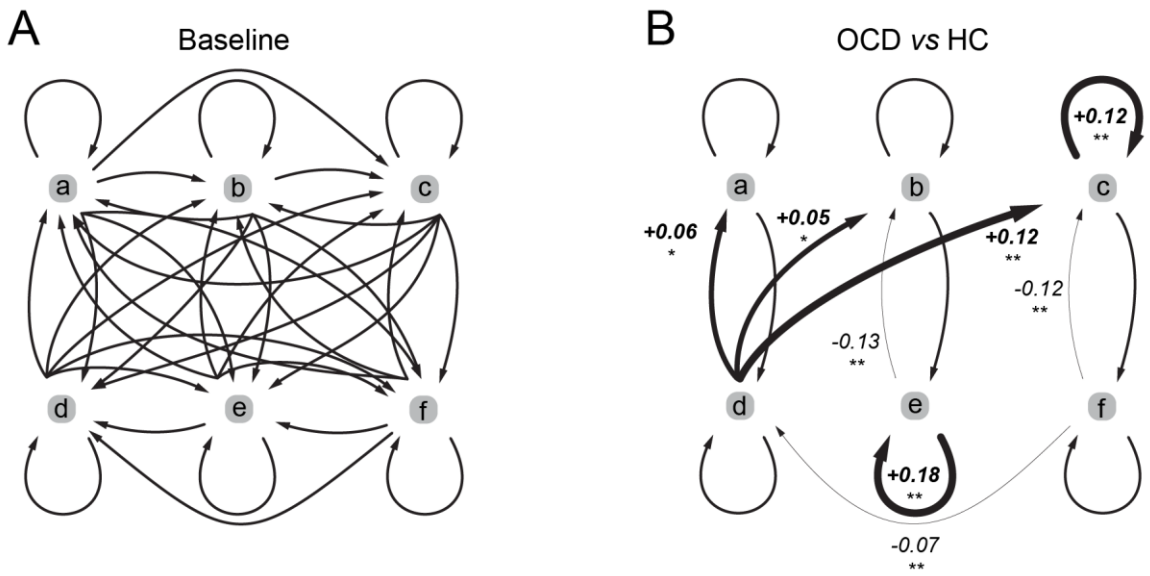

Supplementary Figure 3: Fully connected DCM. (A) Fully connected model, comprising all possible within and between region couplings. Note that the dorsal caudate and related frontal region were excluded from this analysis because of the lack of significant cluster in functional connectivity between groups. **(B)** Changes of coupling associated to OCD pathology. Note that cross-pathways arrows were removed of the illustration for clarity when they do not differ between groups. Posterior probabilities: *Pp>0.7, **Pp>0.99. a: orbitofrontal cluster, b: lateral prefrontal cluster, c: dorsal prefrontal cluster, d: nucleus accumbens, e: dorsal putamen, and f: ventral putamen.

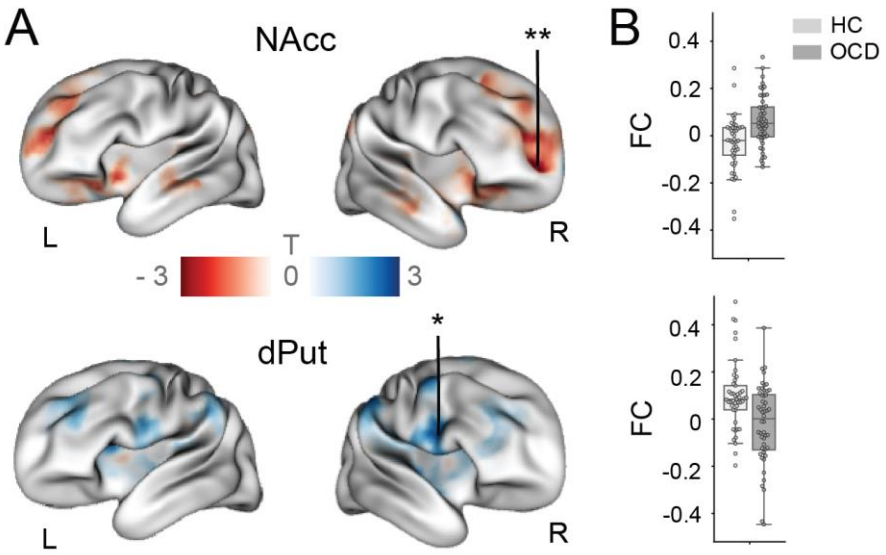

Supplementary Figure 4: Functional connectivity differences in OCD versus healthy controls (HC) using cortical masks derived from the Human Connectome Project. (A) Main effect of group: increased (red) and decreased (blue) functional connectivity in OCD compared to healthy controls. * p_{FWE}=0.04, ** p_{FWE}=0.03. NAcc: nucleus accumbens seed (MNI coordinates [x,y,z] = [±9, 9, -8]); dPut: dorsal putamen seed ([±28, 1, 3]); R: Right hemisphere; L: Left hemisphere. **(B)** Pearson correlation values (FC) between fMRI signals in the seed regions and the highlighted clusters denoted by asterisks in panel A. Boxes extend from first to third quartile, whiskers span 1.5 of the interquartile range, and individuals' FC are marked by small circles.

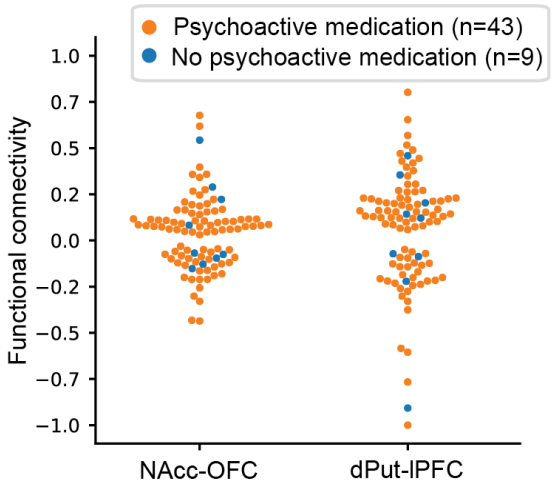

Supplementary Figure 5: Functional connectivity values for participants on and off psychoactive medications. Functional connectivity within each frontostriatal system of interest is displayed for each subject, color-coded according to their medication status during the study.

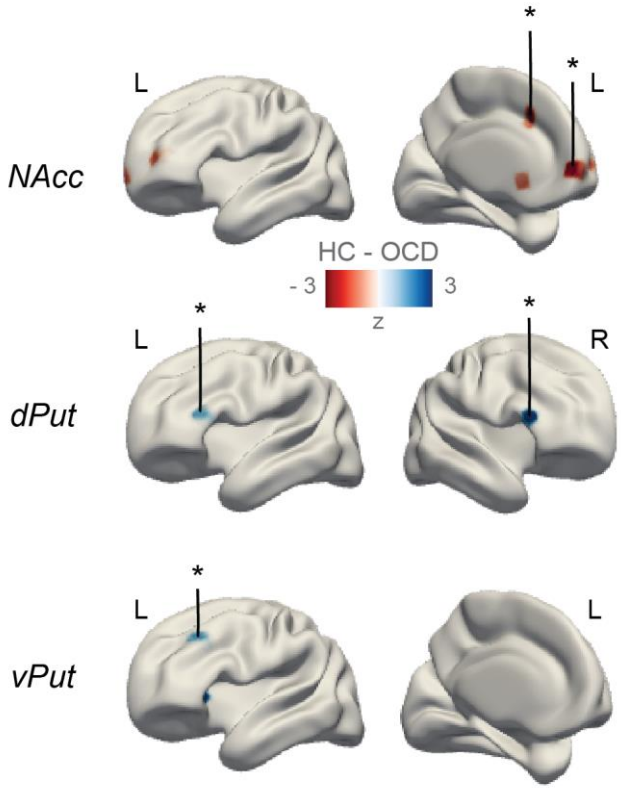

Supplementary Figure 6: Results from previous work assessing changes in resting state frontostriatal functional connectivity. Functional connectivity maps reconstructed from Table 1 in Harrison *et al.*[4] using a 6 mm radius sphere as volume of interest centred at reported cluster locations (NAcc to orbitofrontal cortex (cluster centroids [x,y,z]): [-19,25,-4], [-10, 60, -4], [-29, 49, 3]; NAcc to anterior cingulate cortex: [-7, 27, 34], [-8, 24, -6]; dPut to inferior frontal gyrus: [-43, 32, 7], [51, 33, 8]; vPut to middle frontal gyrus: [-34, 27, -1], [-35, 30, 30]; vPut to inferior frontal gyrus: [-16, 27, 4]; vPut to medial frontal gyrus: [16, 40, -2]). Colour code and scale represent negative (OCD>HC, red) to positive (HC>ODC, blue) z-score statistics (* p_{uncorr}<0.001) as reported in Harrison *et al.*[4].

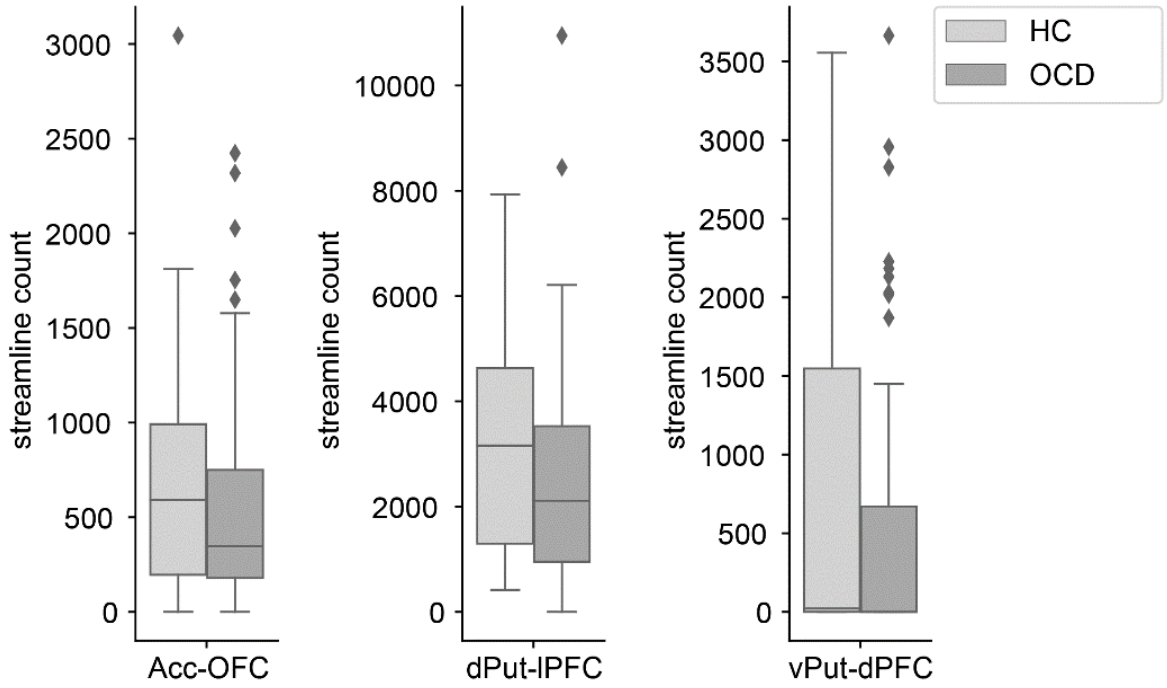

Supplementary Figure 7: Streamline counts in the three pathways of interest. Number of estimated streamlines between the seed regions and their respective functional clusters (identical to the one used in Figure 2A). Horizontal lines in boxes are median of the distribution, and whiskers span from the 25th to the 75th percentiles; losanges show outliers (> 2.3 S.D.). Distributions were not significantly different across groups (2-tailed unpaired t-tests: $T<1.5$, $p>0.15$; confirmed by two-sample Kolmogorov-Smirnov tests $p>0.1$).